ASK1 signaling regulates phase-specific glial interactions during neuroinflammation

Xiaoli Guo[a,1] , Atsuko Kimura[a,1] , Kazuhiko Namekata[a,1] , Chikako Harada[a], Nobutaka Arai[b] , Kohsuke Takeda[c], Hidenori Ichijo[d], and Takayuki Harada[a,2]

[a]Visual Research Project, Tokyo Metropolitan Institute of Medical Science, Tokyo 156-8506, Japan; [b]Brain Pathology Research Center, Tokyo Metropolitan Institute of Medical Science, Tokyo 156-8506, Japan; [c]Department of Cell Regulation, Graduate School of Biomedical Sciences, Nagasaki University, Nagasaki 852-8521, Japan; and [d]Laboratory of Cell Signaling, Graduate School of Pharmaceutical Sciences, The University of Tokyo, Tokyo 113-0033, Japan

Neuroinflammation is well known to be associated with neurodegenerative diseases. Apoptosis signal-regulating kinase 1 (ASK1) is a mitogen-activated protein kinase kinase kinase that has been implicated in neuroinflammation, but its precise cellular and molecular mechanisms remain unknown. In this study, we generated conditional knockout (CKO) mice that lack ASK1 in T cells, dendritic cells, microglia/macrophages, microglia, or astrocytes, to assess the roles of ASK1 during experimental autoimmune encephalomyelitis (EAE). We found that neuroinflammation was reduced in both the early and later stages of EAE in microglia/macrophage-specific ASK1 knockout mice, whereas only the later-stage neuroinflammation was ameliorated in astrocyte-specific ASK1 knockout mice. ASK1 deficiency in T cells and dendritic cells had no significant effects on EAE severity. Further, we found that ASK1 in microglia/macrophages induces a proinflammatory environment, which subsequently activates astrocytes to exacerbate neuroinflammation. Microglia-specific ASK1 deletion was achieved using a *CX3CR1^CreER* system, and we found that ASK1 signaling in microglia played a major role in generating and maintaining disease. Activated astrocytes produce key inflammatory mediators, including CCL2, that further activated and recruited microglia/macrophages, in an astrocytic ASK1-dependent manner. Astrocyte-specific analysis revealed CCL2 expression was higher in the later stage compared with the early stage, suggesting a greater proinflammatory role of astrocytes in the later stage. Our findings demonstrate cell-type–specific roles of ASK1 and suggest phase-specific ASK1-dependent glial cell interactions in EAE pathophysiology. We propose glial ASK1 as a promising therapeutic target for reducing neuroinflammation.

glial interactions | neuroinflammation | microglia | astrocyte | ASK1

Apoptosis signal-regulating kinase 1 (ASK1) is a mitogen-activated protein kinase (MAPK) kinase kinase that stimulates the c-Jun N-terminal kinase (JNK) and p38 MAPK pathways, and it mediates diverse biological signals leading to cell death, differentiation, and senescence (1, 2). Deletion of ASK1 in mice suppresses neuronal cell death from injury (3, 4), and recent studies indicate that ASK1 is involved in various neurodegenerative diseases, including amyotrophic lateral sclerosis, Alzheimer's disease, Parkinson's disease, and multiple sclerosis (MS) (5–8). MS is an inflammatory disease of the central nervous system (CNS) characterized by localized areas of demyelination. Experimental autoimmune encephalomyelitis (EAE) is a classic model widely used to explore pathogenic mechanisms of MS, generated by administering a myelin basic protein peptide that induces an autoimmune response directed to myelin (9). During MS/EAE, activated microglia/macrophages are the first cells to respond to inflammatory insults within the CNS. Microglia/macrophages may be polarized into proinflammatory or antiinflammatory states, with each state having a distinct molecular phenotype and effector function, and targeting microglia/macrophages may have therapeutic benefits in MS/EAE treatment (10–12). Astrocytes, another

subset of glia, are the most abundant cell population within the CNS. Astrocytes are involved in the regulation of synaptic function, plasticity, and maintaining brain homeostasis, and they are thought to contribute to the pathogenesis of MS/EAE by producing proinflammatory cytokine/chemokines such as CCL2 (13–16). In recent years, astrocytes have also been shown to polarize into different subtypes: A1 astrocytes are neurotoxic, and blocking the conversion of astrocytes into the A1 phenotype is neuroprotective (17, 18); although, nowadays, the activation state is described to be more diverse than the simple A1/A2 nomenclature (19, 20). Studies of intrinsic and external factors involved in astrocyte activation or polarization may provide information regarding how astrocytic function changes during disease, which may lead to the development of novel therapies.

We previously reported that ASK1 deficiency ameliorated the severity of EAE, using conventional ASK1 knockout (ASK1 KO) mice (21). In this study, we selectively deleted ASK1 from five types of cells: T cells, dendritic cells, microglia/macrophages, microglia, and astrocytes, to dissect out the roles of ASK1 in different cell types during neuroinflammation. Our study revealed pathogenic roles of ASK1 signaling in innate immune cells and how they interact with each other in the progression of MS/EAE.

Significance

Neuroinflammation is associated with many neurodegenerative diseases such as Alzheimer's disease and multiple sclerosis (MS). Thus, decreasing neuroinflammation may be a promising treatment for these diseases. Apoptosis signal-related kinase 1 (ASK1) has been shown to cause neuroinflammation in neurodegenerative disease models, but its mechanism of action has been unclear. Here, we generated conditional knockout mice that lack ASK1 in T cells, dendritic cells, microglia/macrophages, microglia, or astrocytes, to assess the roles of ASK1 during experimental autoimmune encephalomyelitis (EAE), a mouse model of MS. We propose that ASK1 is required in microglia and astrocytes to cause and maintain neuroinflammation by a feedback loop between these two cell types.

[1]X.G., A.K., and K.N. contributed equally to this work.

[2]To whom correspondence may be addressed. Email: harada-tk@igakuken.or.jp.

NEUROSCIENCE

Results

Cell-Type–Specific Roles of ASK1 Signaling in EAE Progression and Severity.

To elucidate the cell-type–specific role of ASK1 signaling during neuroinflammation, we examined myelin oligodendrocyte glycoprotein (MOG)-induced EAE susceptibility in ASK1 conditional knockout (CKO) mice. ASK1$^{flox/flox}$ mice (22) were crossed with *Lck-Cre$^+$*, *Cd11c-Cre$^+$*, *LysM-Cre$^+$*, or *GFAP-Cre$^+$* mice to generate T cell-, dendritic cell-, microglia/macrophage-, or astrocyte-specific CKO lines (Fig. 1*A*). The resulting double-transgenic mice, ASK1$^{flox/flox}$;*Lck-Cre$^+$* (ASK1^{Lck} KO), ASK1$^{flox/flox}$;*Cd11c-Cre$^+$* (ASK1^{Cd11c} KO), ASK1$^{flox/flox}$;*LysM-Cre$^+$* (ASK1^{LysM} KO), and ASK1$^{flox/flox}$;*GFAP-Cre$^+$*(ASK1^{GFAP} KO) were all viable and fertile. Since daily clinical scores of wild-type (WT) EAE mice were similar to those of ASK1$^{flox/flox}$ EAE mice, we show the data of WT EAE mice.

As shown in Fig. 1*B*, the severity of paralytic symptoms in ASK1^{Lck} KO EAE and ASK1^{Cd11c} KO EAE mice were comparable to WT EAE mice, indicating that ASK1 deficiency in T cells and dendritic cells has very little effect on neuroinflammation in EAE. These findings are consistent with results from our previous study, which demonstrated that ASK1 deficiency had no effect on the proliferation of T cells and the polarization of naïve T cells (21). On the other hand, the clinical symptoms observed in ASK1^{LysM} KO EAE and ASK1^{GFAP} KO EAE mice were ameliorated compared with WT EAE mice. The ASK1^{LysM} KO EAE mice demonstrated a similar disease profile to ASK1 KO EAE mice, while ASK1^{GFAP} KO EAE mice only showed a reduction in clinical scores during the later stage of the disease (from day 23 after MOG immunization) (Fig. 1*B*). Consistent with the reduced clinical scores, the extent of demyelination was drastically reduced in ASK1^{LysM} KO EAE, ASK1^{GFAP} KO EAE, and ASK1 KO EAE mice, while the extent of demyelination in ASK1^{Lck} KO EAE and ASK1^{Cd11c} KO EAE mice was similar to that found in WT EAE mice (Fig. 1 *C* and *D*). In support of these results, immunoreactivity for phosphorylated ASK1 (p-ASK1) and phosphorylated p38 (p-p38), which acts downstream of ASK1, were colocalized with iba1 and GFAP, cell markers for microglia/macrophages and astrocytes, in the spinal cords of WT EAE mice (*SI Appendix,* Fig. S1).

We also examined the effects of cell-type–specific deletion of ASK1 on the severity of optic neuritis, characterized by inflammation of the optic nerve, in the above EAE mice. Similar to the results seen in the ASK1 KO EAE mice, the levels of demyelination observed in the optic nerves of ASK1^{LysM} KO EAE and ASK1^{GFAP} KO EAE mice were milder than the level of demyelination found in WT EAE mice (Fig. 1 *E* and *F*). Analysis of semithin and ultrathin sections of the optic nerve revealed many degenerated axons in WT EAE mice, but not in ASK1^{LysM} KO EAE and ASK1^{GFAP} KO EAE mice (Fig. 1*G*). Taken together, these data indicate that ASK1 signaling in microglia/macrophages and astrocytes play important and distinct roles during EAE.

ASK1 Signaling Is Critical for Proinflammatory Microglia/Macrophage Polarization.

To determine the mechanisms to explain the reduced disease severity observed in ASK1^{LysM} KO EAE mice, we first compared the cell number of microglia/macrophage in the spinal cord of naïve ASK1^{LysM} KO mice with that of naïve WT mice. No difference of iba1 positive microglia/macrophage was found between the two genotypes (*SI Appendix,* Fig. S2), indicating that ASK1 signaling is unnecessary to main homeostasis of microglia/macrophages. We then investigated the cell number of microglia/macrophage during the presymptomatic phase of EAE. Iba1-positive cells were significantly increased in both WT and ASK1^{LysM} KO EAE, and there was no difference

in the cell numbers between the two genotypes (*SI Appendix,* Fig. S3). Moreover, the size of the GFAP-positive areas in WT was similar to ASK1^{LysM} KO EAE. In addition, no neuronal loss was observed in this EAE phase and there was no difference in the numbers of NeuN-positive neurons between the two genotypes (*SI Appendix,* Fig. S3). Since vascular remodeling occurs ahead of the EAE disease onset and is a central component of demyelinating diseases (23, 24), we also investigated the effect of ASK1 deficiency in microglia/macrophage on vascular remodeling by studying CD31-positive endothelial cells and the expression of fibronectin, an extracellular matrix protein (*SI Appendix,* Fig. S4). The CD31- or fibronectin-positive area was increased in WT and ASK1^{LysM} KO EAE mice before disease onset, and there was no difference between the two genotypes (*SI Appendix,* Fig. S4). Taken together, these results indicate that ASK1 deficiency in microglia/macrophage has no effect on glial cells, neurons, or vascular remodeling during early presymptomatic phases of EAE.
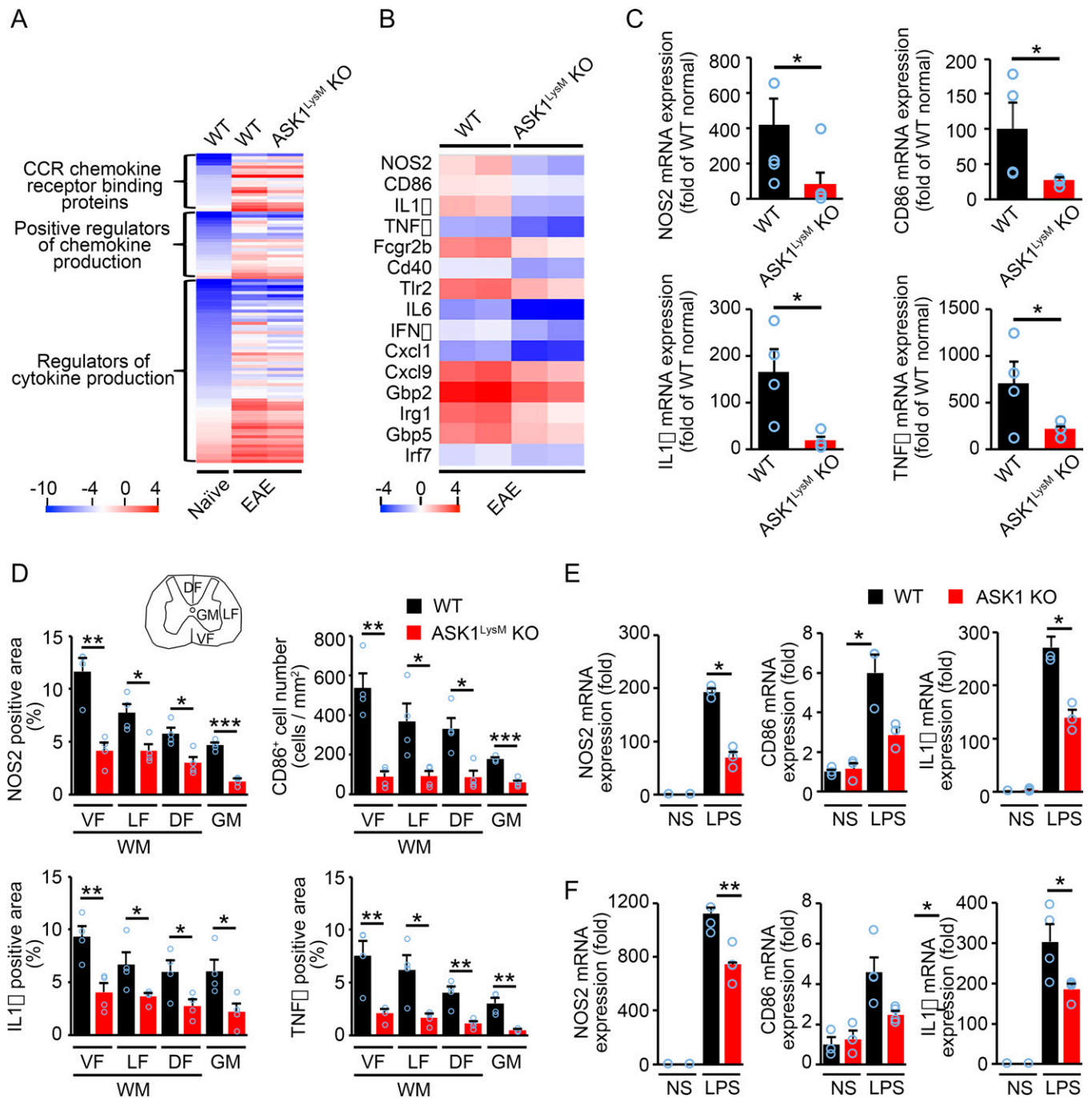
We next performed microarray analysis using mRNAs isolated from the spinal cords on day 17 (d17) when the severity of EAE in ASK1^{LysM} KO mice significantly decreased. When the genome-wide global gene expression profiles were obtained, the results revealed 4,816 cases of gene up-regulation (>2-fold) and 3,273 cases of gene suppression (<0.5-fold) in WT EAE mice compared with naïve WT mice. We focused on the up-regulated genes and analyzed gene ontology using Gene-Spring 14.5 software. Of the 4,816 genes that were up-regulated by >2-fold, a total of 101 genes were related to proinflammatory cytokine/chemokine signaling. Their expression levels were reduced markedly in ASK1^{LysM} KO EAE mice compared with WT EAE mice (Fig. 2*A*). We found that classical proinflammatory microglia/macrophage-related genes, including NOS2, CD86, IL-1β, and TNFα, were all decreased in the spinal cords of ASK1^{LysM} KO EAE mice compared with WT EAE mice (Fig. 2*B*). To confirm the microarray analysis data, we also evaluated gene expression in the spinal cords of WT and ASK1^{LysM} KO EAE mice on d17 using qPCR. Expression levels of NOS2, CD86, IL-1β, and TNFα were all reduced significantly in ASK1^{LysM} KO EAE mice compared with WT EAE mice (Fig. 2*C*). Furthermore, we investigated the expression of these four important genes in different areas of the spinal cord by immunohistochemical staining on d17 (Fig. 2*D* and *SI Appendix,* Fig. S5). Their expression levels were all significantly reduced in the spinal cords of ASK1^{LysM} KO EAE mice, in both the white matter (ventral, lateral, and dorsal funiculus) and gray matter. These results show that the changes in the gene expression matched the changes in protein expression, and that ASK1 deletion in microglia/macrophage reduced expression of NOS2, CD86, IL1β, and TNFα all across the areas in the EAE spinal cord. However, since the cell number of microglia/macrophage was reduced in ASK1^{LysM} KO EAE mice on d17 (*SI Appendix,* Fig. S6), it is not clear whether the reduced gene expressions might be due to the overall reduction of cell numbers or they reflect reduced gene expressions per cell. Therefore, to prove that ASK1 signaling regulates the production of classical proinflammatory microglia/macrophage-related genes, we stimulated primary cultured microglia or bone marrow–derived macrophages (BMDMs) from WT and ASK1 KO mice with lipopolysaccharide (LPS; 100 ng/mL for proinflammatory polarization) for 6 h. At 6 h after LPS stimulation, the expression of NOS2, CD86, and IL-1β was reduced in microglia or BMDMs with ASK1 deficiency (Fig. 2 *E* and *F*). We also determined whether ASK1 affects polarization of microglia/macrophages toward an antiinflammatory phenotype. For this, we stimulated cultured microglia or BMDMs from WT and ASK1 KO mice with IL-4 (20 ng/mL) to induce an antiinflammatory phenotype and examined levels of antiinflammatory microglial/macrophage markers. The results of this experiment showed
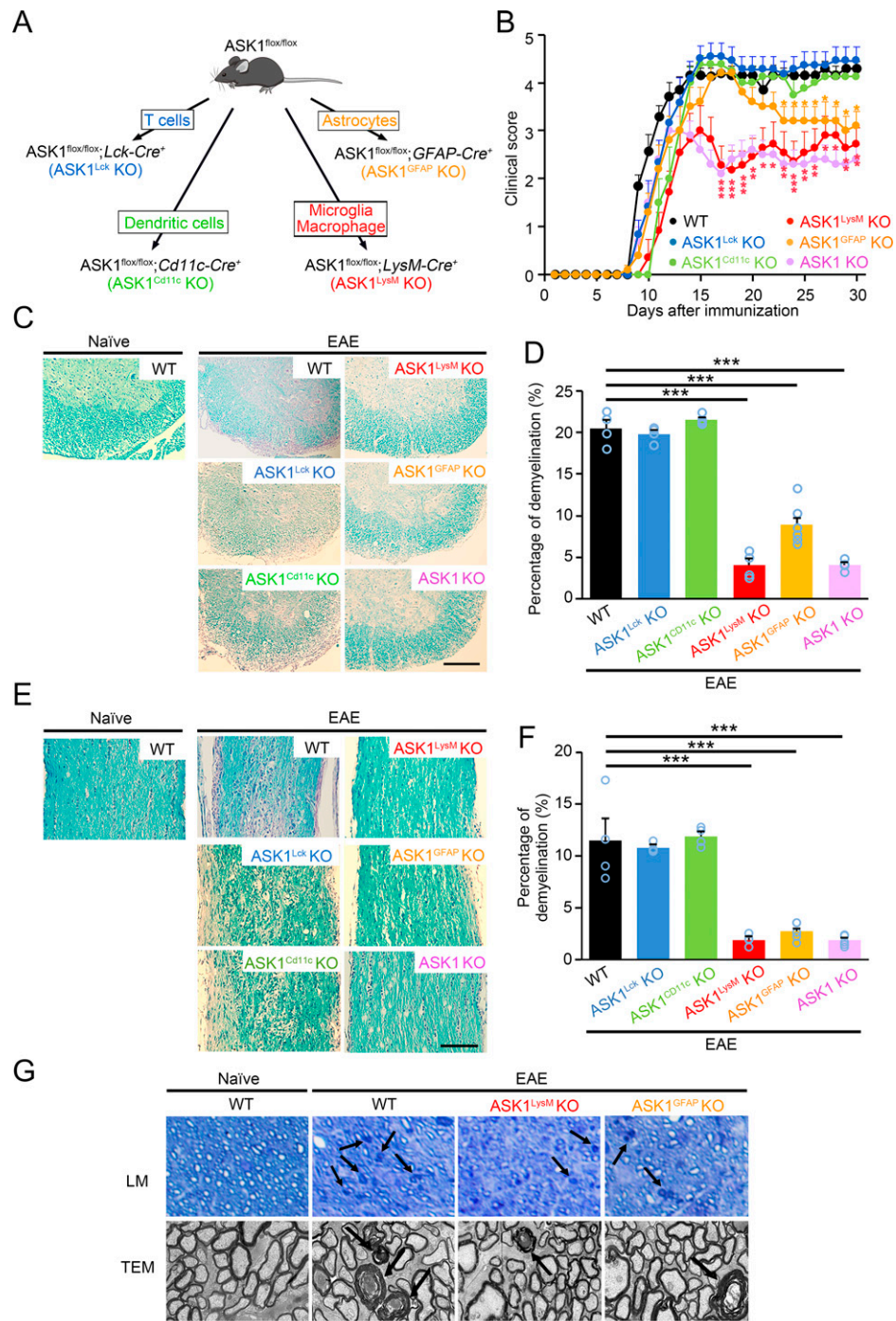
Fig. 1. Selective ASK1 deletion in microglia/macrophages or astrocytes reduced the severity of EAE. (*A*) Schematic diagram illustrating the breeding strategy and experimental design for cell-specific ASK1 knockout in T cells (*Lck-Cre*[+]), dendritic cells (*Cd11c-Cre*[+]), microglia/macrophages (*LysM-Cre*[+]), and astrocytes (*GFAP-Cre*[+]). (*B*) Clinical scores of wild-type (WT; $n = 15$), ASK1[Lck] KO ($n = 12$), ASK1[Cd11c] KO ($n = 8$), ASK1[LysM] KO ($n = 11$), ASK1[GFAP] KO ($n = 19$), and ASK1 conventional KO ($n = 8$) EAE mice in a period of 30 d after MOG immunization (d30). The one-way ANOVA with Tukey–Kramer post hoc test was used. ***$P < 0.001$; **$P < 0.01$; *$P < 0.05$. (*C*) Spinal cord sections of naïve WT and six lines of EAE mice were stained with LFB and H&E. (Scale bar: 250 μm.) (*D*) Quantitative analysis regarding the extent of demyelination in the spinal cords of the six lines of EAE mice. The one-way ANOVA with Tukey–Kramer post hoc test was used. $n = 4$ to 6 mice per group. ***$P < 0.001$. (*E*) Histopathology of the optic nerves of normal WT and six lines of EAE mice. Optic nerve sections were stained with LFB and H&E. (Scale bar: 170 μm.) (*F*) Quantitative analysis regarding the extent of demyelination in the optic nerves of the six lines of EAE mice. The one-way ANOVA with Tukey–Kramer post hoc test was used. $n = 4$ to 6 mice per group. ***$P < 0.001$. (G) Axonal degeneration in the optic nerves as observed in semithin sections by the light microscope (LM) and ultrathin sections by transmission electron microscope (TEM). Arrows point to representative degenerated axons. (Scale bar: 45 μm, *Upper* and 2.5 μm, *Lower*.)

that ASK1 signaling in microglia/macrophages is not involved in promoting or inhibiting polarization of microglia/macrophages toward an antiinflammatory phenotype (*SI Appendix,* Fig. S7). These data indicated that ASK1 promotes a proinflammatory phenotype in microglia/macrophages. We also examined T cell infiltration to the lesion site in ASK1[LysM] KO

Guo et al.
ASK1 signaling regulates phase-specific glial interactions during neuroinflammation

PNAS | 3 of 12
https://doi.org/10.1073/pnas.2103812119

Fig. 2. ASK1 is involved in proinflammatory microglia/macrophage polarization. (*A*) Cytokines/chemokines revealed by microarray analysis of spinal cords from normal, WT EAE, and ASK1^{LysM} KO EAE mice on d17. (*B*) Heat map of the changes in expression for proinflammatory microglia/macrophage-related genes (fold change >2.0) in the spinal cords of ASK1^{LysM} KO EAE mice compared with WT EAE mice (*n* = 2) on d17 after MOG immunization. (*C*) qPCR analysis of proinflammatory microglia/macrophage-related gene expressions in the spinal cords of WT EAE and ASK1^{LysM} KO EAE mice on d17. The one-way ANOVA with Tukey–Kramer post hoc test was used. *n* = 4 to 6 mice per group. *P < 0.05. (*D*) Quantification of NOS2-, CD86-, IL1β-, and TNFα-positive stained areas in the ventral funiculus (VF), lateral funiculus (LF), dorsal funiculus (DF) of the white matter (WM), and gray matter (GM) in the spinal cords of WT and ASK1^{LysM} KO EAE mice on d17. Student's *t* test was used. *n* = 4 for WT EAE mice and ASK1^{LysM} KO EAE mice, respectively. ***P < 0.001. **P < 0.01; *P < 0.05. (*E* and *F*) mRNA expression of proinflammatory microglia/macrophage-related genes in WT and ASK1 KO microglia (*E*) or macrophage (*F*) stimulated with LPS (100 ng/mL) for 6 h. NS: nonstimulated. Experiments were carried out in a 96-well plate format with three to four wells used for each culture condition. Experiments were repeated three times and representative results are shown. Two-tailed Student's *t* test was used. **P < 0.01; *P < 0.05.

EAE mice and found that there was no difference in T cell numbers between WT and ASK1^{LysM} KO EAE mice, indicating that ASK1 deficiency in microglia/macrophages had no effect on T cell infiltration (*SI Appendix*, Fig. S6).

ASK1 Deficiency in Microglia Mimics the Phenotype Observed in ASK1^{LysM} KO EAE Mice. We elucidated the role of ASK1 in microglia/macrophages using the *LysM-Cre* line, which cannot distinguish between microglia and macrophages. Thus, roles of
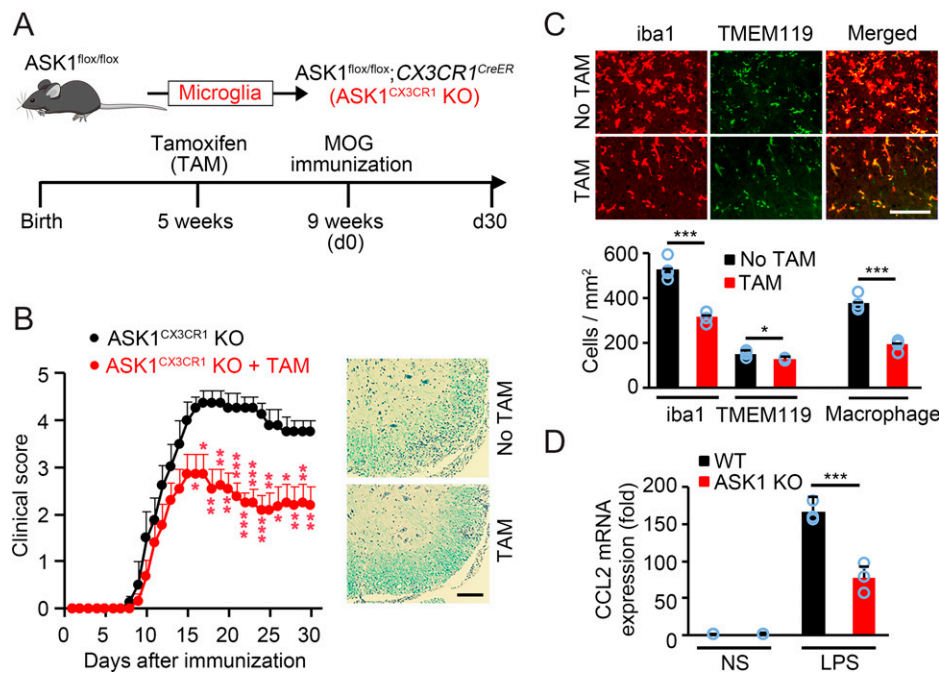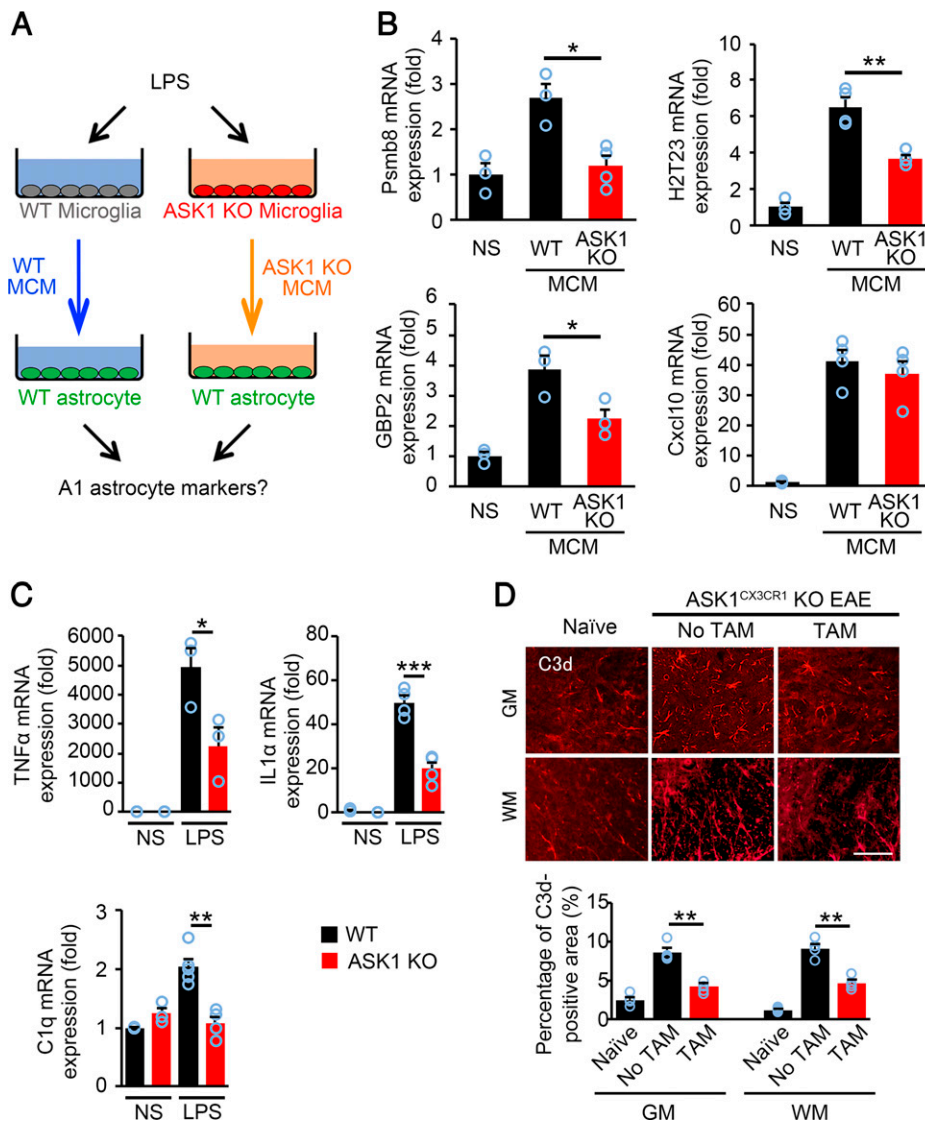
Fig. 3. ASK1 deficiency in microglia nearly reproduced the phenotype observed in ASK1^{LysM} KO mice. (*A*) Schematic diagram illustrating the breeding strategy and experimental design for cell-specific ASK1 knockout in microglia (ASK1^{CX3CR1} KO). (*B*) Clinical scores of ASK1^{CX3CR1} KO EAE mice with or without preadministered TAM (*n* = 13 and *n* = 8, respectively). Representative spinal cord sections stained with LFB and H&E are shown at *Right*. Two-tailed Student's *t* test was used. ***P < 0.001; **P < 0.01; *P < 0.05. (Scale bar: 100 μm.) (*C*) Immunohistochemical staining of iba1 and TMEM119 in the white matter of the spinal cords of ASK1^{CX3CR1} KO EAE mice killed on their EAE onset day. Quantitative analysis of iba1-positive and TMEM119-positive cells is shown (*Lower*). Macrophage numbers were deduced from iba1-positive microglia/macrophage and TMEM119-positive microglia numbers. Two-tailed Student's *t* test was used. *n* = 4 mice per group. ***P < 0.001. *P < 0.05. (Scale bar: 100 μm.) (*D*) mRNA expression of CCL2 in WT and ASK1 KO microglia stimulated with LPS (100 ng/mL) for 6 h. NS: nonstimulated. Experiments were carried out in a 96-well plate format with 3 wells used for each culture condition. Experiments were repeated three times and representative results are shown. Two-tailed Student's *t* test was used. ***P < 0.001.

ASK1 in microglia or in macrophages during EAE remain unknown. To examine the role of ASK1 specifically in microglia, we crossed ASK1$^{flox/flox}$ mice with *CX3CR1*^{CreER} mice (ASK1^{CX3CR1} KO, Fig. 3*A*) and induced microglia-specific gene deletion as previously reported (25). We first confirmed microglia-specific gene manipulation using Tomato$^{flox/flox}$; *CX3CR1*^{CreER} transgenic (Tomato^{CX3CR1} Tg) EAE mice (*SI Appendix*, Fig. S8*A*) and the microglia marker TMEM119 (*SI Appendix*, Fig. S8*B*). Moreover, ASK1 immunohistochemistry staining revealed that ASK1 was hardly detectable in microglia in the spinal cords of ASK1^{CX3CR1} KO EAE mice preadministered with tamoxifen (TAM) (*SI Appendix*, Fig. S8*C*). We then compared severities of ASK1^{CX3CR1} KO EAE mice with or without TAM preadministration. As shown in Fig. 3*B*, EAE severity was significantly reduced from the early stage in ASK1^{CX3CR1} KO mice with preadministered TAM compared with mice without TAM administration, which is accompanied by lower extent of demyelination and decreased cell infiltration in the spinal cords, as demonstrated by luxol fast blue (LFB) and hematoxylin and eosin (H&E) staining. These results are similar to what we found in ASK1^{LysM} KO EAE mice, suggesting that ASK1 in microglia may play a major role in the pathogenesis of EAE.

In the context of injury, microglia are activated prior to the arrival of macrophages and may actively participate in their recruitment (26), which might also be the case during EAE. We then compared cell numbers of microglia and macrophages in the spinal cords of ASK1^{CX3CR1} KO EAE mice with or without preadministered TAM at EAE onset (Fig. 3*C*). Macrophage numbers were deduced from iba1-positive microglia/macrophage numbers and TMEM119-positive microglia numbers. While there was only a slight reduction of microglia numbers in

ASK1^{CX3CR1} KO EAE mice with preadministered TAM compared with mice without TAM administration (128 ± 3 vs. 153 ± 7, P = 0.0149), the numbers of macrophages were drastically reduced (193 ± 13 vs. 378 ± 17, P = 0.000146; Fig. 3*C*). In addition, we found that expression of CCL2, a chemokine that recruits macrophages (27), was significantly reduced in ASK1-deficient microglia upon LPS stimulation (Fig. 3*D*). Immunoblot analysis confirmed reduced p-p38 expression in ASK1-deficient microglia stimulated with LPS or CpG, a ligand of TLR9 (*SI Appendix*, Fig. S9), suggesting that the effects may be mediated via TLR9 as well as TLR4. These results suggest that microglial ASK1 is involved in macrophage recruitment to the lesion site.

ASK1 Signaling in Microglia Stimulates the Induction of an A1 Phenotype in Astrocytes. A1 astrocytes, a subtype of reactive astrocytes, are induced by proinflammatory mediators released from microglia (17). Since ASK1 is involved in the polarization of microglia toward the proinflammatory phenotype, we determined whether ASK1 signaling in microglia mediates the induction of the A1 phenotype in astrocytes. To test this hypothesis, we prepared microglial conditioned medium (MCM) by stimulating WT and ASK1-deficient microglia with LPS. WT astrocytes were exposed to MCM from WT and ASK1-deficient microglia, and qPCR was used to measure levels of A1 markers in astrocytes (Fig. 4*A*). The expression of the A1 astrocyte markers *Psmb8*, *H2T23*, and *GBP2* were significantly decreased in WT astrocytes stimulated with MCM from ASK1 KO microglia compared with those stimulated with MCM from WT microglia (Fig. 4*B*). However, levels of the pan-reactive astrocyte marker, *Cxcl10*, remained comparable between WT astrocytes stimulated with MCM from ASK1 KO microglia and those stimulated with MCM from WT microglia, demonstrating

Guo et al.
ASK1 signaling regulates phase-specific glial interactions during neuroinflammation

PNAS | 5 of 12
https://doi.org/10.1073/pnas.2103812119

NEUROSCIENCE

Fig. 4. ASK1 deficiency in microglia reduced induction of A1 astrocytes in vitro and in vivo. (*A*) Schematic representation of the experimental procedure for A1 astrocyte induction. (*B*) A1 astrocyte marker expression (Psmb8, H2T23, and GBP2) in WT astrocytes stimulated with WT MCM or ASK1-deficient MCM for 6 h. The expression of Cxcl10, one of pan-reactive astrocyte markers, was also quantified. Experiments were carried out in a 96-well plate format with 3 to 4 wells used for each culture condition. Experiments were repeated three times and representative results are shown. The one-way ANOVA with Tukey–Kramer post hoc test was used. **$P < 0.01$; *$P < 0.05$. (*C*) TNFα, IL1α, and C1q mRNA expression in WT and ASK1 KO microglia stimulated with LPS (100 ng/mL) for 6 h. NS: nonstimulated. Experiments were carried out in a 96-well plate format with 3 to 4 wells used for each culture condition. Experiments were repeated three times and representative results are shown. Two-tailed Student's *t* test was used. ***$P < 0.001$; **$P < 0.01$; *$P < 0.05$. (*D*) Immunohistochemical staining of C3d in the gray matter (GM) and white matter (WM) of the spinal cords of ASK1^{CX3CR1} KO EAE mice with or without preadministered TAM on d30 and quantification of the C3d-positive area. The one-way ANOVA with Tukey–Kramer post hoc test was used. $n = 4$ for WT normal group, $n = 6$ for ASK1^{CX3CR1} KO EAE group with or without TAM preadministration. **$P < 0.01$. (Scale bar: 60 μm.)

that the number of total astrocytes is similar between the two groups (Fig. 4*B*). We also found that stimulation of WT microglia with LPS up-regulated the expression of TNFα, IL-1α, and C1q, factors that induce the A1 phenotype in astrocytes. However, these effects were all significantly reduced in ASK1-deficient microglia compared to WT microglia (Fig. 4*C*). Immunohistochemical analysis of C3d, a marker of A1 astrocytes, demonstrated that the number of A1 astrocytes was significantly reduced in both the gray matter and white matter of the spinal cord of ASK1^{CX3CR1} KO EAE mice with preadministered TAM compared with mice without TAM administration (Fig. 4*D*). Together, these data indicate that ASK1 signaling in microglia promotes induction of the A1 phenotype in astrocytes during neuroinflammation.

ASK1 Signaling in Astrocytes Is Involved in the Later Stage of EAE Pathophysiology. We have determined that ASK1 signaling in astrocytes regulates the severity of EAE during the later stage of the disease, but not the early stage (Fig. 1*B*). First, we compared the percentage of the GFAP-positive area in the spinal cord of naïve ASK1^{GFAP} KO mice with that in naïve WT mice. No difference was found between the two genotypes (*SI Appendix*, Fig. S10), indicating that ASK1 signaling is unnecessary to maintain homeostasis of astrocytes. Moreover, ASK1 deficiency in astrocytes had no effects on the number of iba1- or GFAP-positive glial cells or NeuN-positive neurons (*SI Appendix*, Fig. S11) or the expression levels of vascular remodeling markers, as demonstrated with CD31- and fibronectin-positive areas during the presymptomatic phase of EAE (*SI*
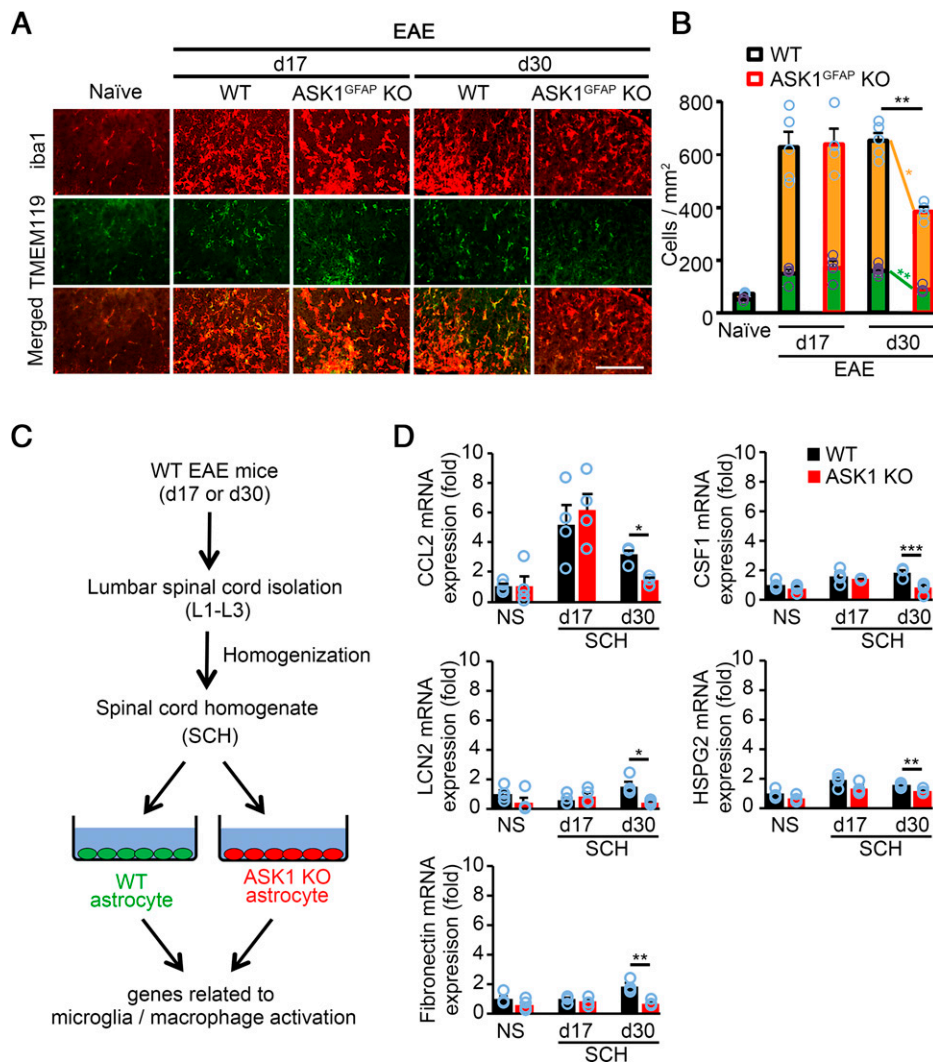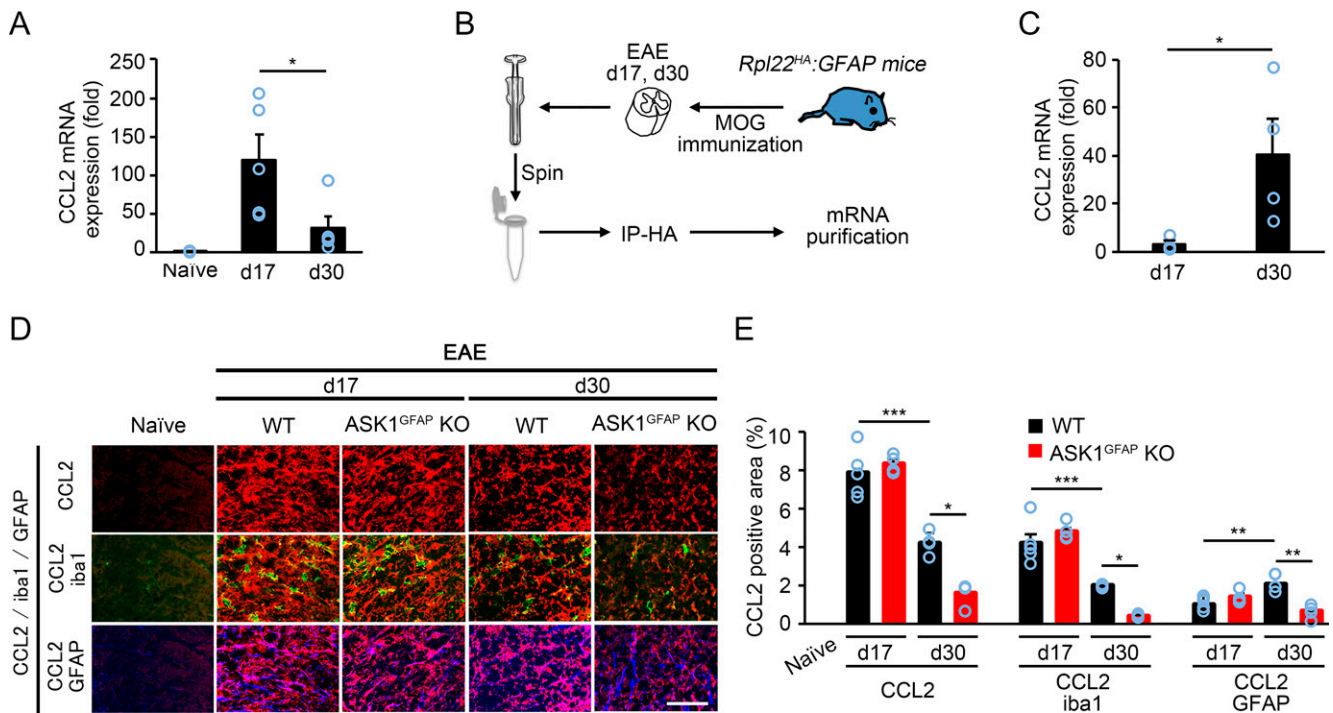
Fig. 5. Lack of ASK1 signaling in astrocytes reduces factors that stimulate microglia/macrophage recruitment and activation at d30, but not d17. (*A*) Immunohistochemical staining of iba1 and TMEM119 in the spinal cords of WT and ASK1^{GFAP} KO EAE mice on d17 and d30. (Scale bar: 100 μm.) (*B*) Quantification of microglia (green bars) and macrophage (yellow bars) cell numbers in the white matter of the spinal cords. Macrophage numbers were deduced from iba1-positive microglia/macrophage and TMEM119-positive microglia numbers. Two-tailed Student's *t* test was used. *n* = 4 to 5 mice per group. **$P < 0.01$; *$P < 0.05$. (*C*) Schematic representation of the experimental procedure. SCHs taken from WT EAE mice on d17 and d30 were used to stimulate astrocytes. (*D*) qPCR analysis of CCL2, CSF1, LCN2, HSPG2, and fibronectin in WT and ASK1 KO astrocytes stimulated with 25 μg/mL of SCH for 6 h. Experiments were carried out in a 96-well plate format with 3 to 4 wells used for each culture condition. Experiments were repeated three times and representative results are shown. Two-tailed Student's *t* test was used. ***$P < 0.001$; **$P < 0.01$; *$P < 0.05$.

Appendix, Fig. S12). We next investigated whether ASK1 signaling in astrocytes was involved in the induction of the A1 phenotype. To test this hypothesis, we performed similar experiments to Fig. 4*A*, but using WT and ASK1 KO astrocytes stimulated with MCM from WT microglia (*SI Appendix*, Fig. S13*A*). We found no significant difference in the expression levels of A1 astrocyte markers between MCM-stimulated WT astrocytes and ASK1 KO astrocytes (*SI Appendix*, Fig. S13*B*). These data indicated that ASK1 signaling in astrocytes is not involved in the polarization of astrocytes toward an A1 phenotype.

We then investigated the potential effects of astrocytic ASK1 signaling on microglia/macrophage activation by immunohistochemistry staining of the spinal cords (Fig. 5*A*). As shown in Fig. 5*B*, the numbers of iba1-positive and TMEM119-positive microglia and the deduced numbers of macrophages were significantly reduced in ASK1^{GFAP} KO EAE mice on d30 but not on d17, indicating that astrocytic ASK1 signaling stimulates microglia/macrophage recruitment and activation only in the

later stage of EAE. Several factors are known to affect microglia/macrophage recruitment and activation, including CCL2, colony-stimulating factor-1 (CSF1), lipocalin-2 (LCN2), HSPG2, and fibronectin (28–34). Therefore, we compared expression of such factors in WT and ASK1-deficient astrocytes stimulated with spinal cord homogenates (SCHs) from d17 or d30 WT EAE mice (Fig. 5*C*). The expression of CCL2, CSF1, LCN2, HSPG2, and fibronectin in ASK1-deficient astrocytes stimulated with SCHs from d17 EAE mice were similar to that of WT astrocytes. However, expressions of these five factors were significantly down-regulated in ASK1-deficient astrocytes compared with WT astrocytes when stimulated with SCHs from d30 EAE mice (Fig. 5*D*). Taken together, our findings suggest that ASK1 signaling in astrocytes recruits and activates microglia/macrophages in the later stage of EAE, which contributes, at least partly, to maintaining disease.

Among the above factors investigated, CCL2 demonstrated the highest up-regulation, which was suppressed in the

Guo et al.
ASK1 signaling regulates phase-specific glial interactions during neuroinflammation

PNAS | 7 of 12
https://doi.org/10.1073/pnas.2103812119

Fig. 6. CCL2 expression is reduced in the spinal cords of ASK1^{GFAP} KO EAE mice at d30, but not d17. (*A*) qPCR analysis of CCL2 expressions in the spinal cords. Two-tailed Student's *t* test was used. *n* = 4 mice per group. *P < 0.05. (*B*) Schematic representation of the experimental procedure for mRNA purification of astrocytes from the spinal cords of *Rpl22^{HA}:GFAP* EAE mice on d17 and d30. Immunoprecipitation using mouse monoclonal anti-HA antibody (IP-HA) was performed before mRNA purification. (*C*) qPCR analysis of CCL2 expressions in astrocytes. Two-tailed Student's *t* test was used. *n* = 4 mice per group. *P < 0.05. (*D*) Triple immunohistochemical staining of CCL2, iba1, and GFAP in the spinal cords of WT and ASK1^{GFAP} KO EAE mice on d17 and d30. (Scale bar: 50 μm.) (*E*) Quantification of the percentage of CCL2-, CCL2/iba1-, and CCL2/GFAP-positive area in the gray matter of the spinal cord. The one-way ANOVA with Tukey–Kramer post hoc test was used. *n* = 4 to 5 mice per group. ***P < 0.001; **P < 0.01; *P < 0.05.

absence of ASK1 (Fig. 5*D*). Since CCL2 has been reported to play important roles during EAE (35, 36) and might be involved in the reduced severity of ASK1^{GFAP} KO EAE mice in the later stage, we examined the in vivo dynamics of CCL2 during the early and later stages of EAE. qPCR analysis of the whole tissue (spinal cords) in WT EAE mice revealed that CCL2 expression was significantly reduced in the later stage compared with the early stage (Fig. 6*A*). We further examined the in vivo dynamics of astrocytic CCL2 by using *Rpl22^{HA}:G-FAP* mice that were generated by crossing RiboTag mice with *GFAP-Cre$^+$* mice to isolate mRNA of astrocytes (Fig. 6*B*) (37). Interestingly, CCL2 expression in astrocytes was significantly increased at d30 compared with d17 (Fig. 6*C*). These data, in combination with the total CCL2 expression in Fig. 6*A*, suggest that different cell types may be responsible for CCL2 production, depending on the disease stage (early/later). Next, we confirmed the in vivo dynamics of CCL2 in astrocytes and microglia by using triple immunohistochemical staining of the spinal cords (Fig. 6*D*). We determined the percentage of CCL2$^+$ microglia or astrocytes by examining the colocalization of CCL2 and iba1 or GFAP immunoreactivity. In accordance with the qPCR analysis, the total CCL2 immunoreactivity was significantly reduced at d30 (Fig. 6*E*). However, we found that the positive area of CCL2$^+$ astrocytes was up-regulated at d30 in WT EAE mice compared with that at d17, while the positive area of CCL2$^+$ microglia was down-regulated at d30. In addition, CCL2 up-regulation was significantly suppressed in ASK1^{GFAP} KO EAE mice on d30, but not on d17 (Fig. 6*E*). Taken together, these results suggest that astrocytes are the major source of CCL2 during the later stage, whereas microglia are mainly responsible for CCL2 production during the early stage.

Discussion

Investigations involving the use of conditional knockout models provide an in-depth understanding of pathological mechanisms in a cell-specific manner. In the present study, we demonstrated that ASK1 deficiency in microglia or microglia/macrophages reduced clinical scores and impaired the production of proinflammatory cytokines/chemokines from the early stage of EAE through to the end of the experimental period, which is similar to the profile observed in conventional ASK1 KO mice. Our findings indicate pathogenic roles of ASK1 signaling in glial cells and their interactions during neuroinflammation (Fig. 7). The recruitment of proinflammatory microglia/macrophages is thought to contribute to the pathogenesis of MS and other neurodegenerative disorders (38–40). In the present study, we found that genes linked to a proinflammatory microglia/macrophage phenotype were down-regulated in ASK1^{LysM} KO EAE mice. In addition, in vitro experiments with primary cultured microglia/macrophages revealed that ASK1 deficiency reduced proinflammatory gene expression but did not alter antiinflammatory genes. These data suggest that reduced clinical severity, decreased expression of proinflammatory genes, and reduced demyelination may partly be explained by the role of ASK1 in inducing a proinflammatory phenotype in microglia/macrophages. Interestingly, our data from TAM-inducible ASK1^{CX3CR1} KO EAE mice suggest that ASK1 in microglia plays a major role in EAE pathogenesis, but not ASK1 in macrophages. However, CNS macrophages comprise microglia and border-associated macrophages (BAMs) residing in the meninges, choroid plexus, and perivascular spaces (41). The *CX3CR1^{CreER}* system will also target BAMs, and therefore it is possible that ASK1 signaling in BAMS could also contribute to EAE pathogenesis. Thus, development of a macrophage-specific conditional gene knockout system may be
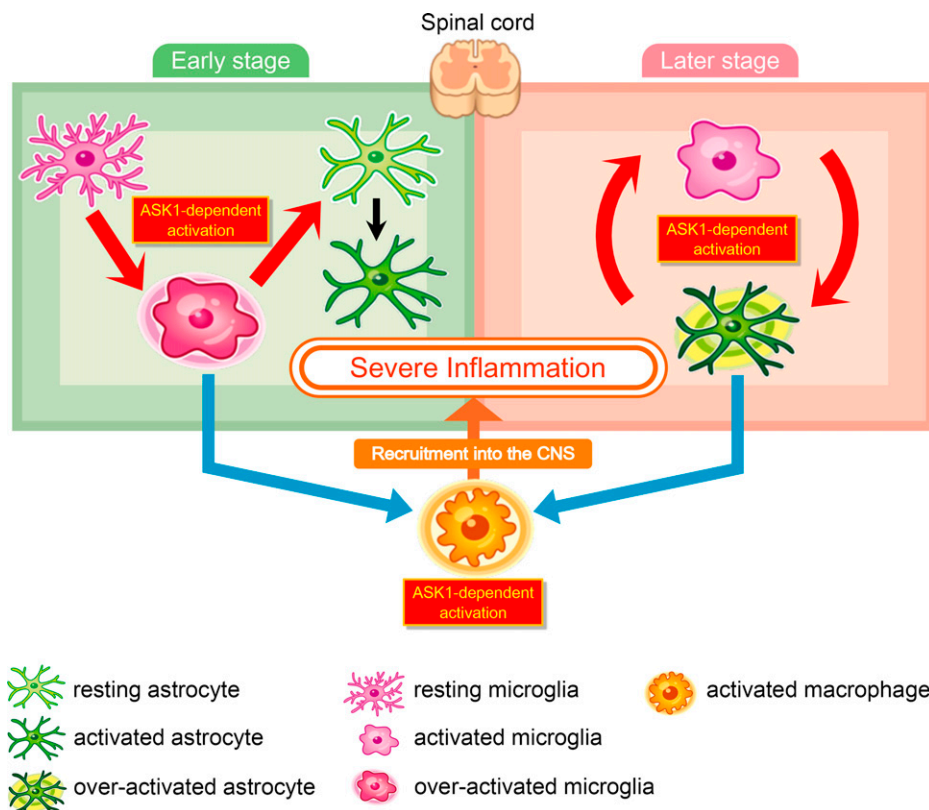
Fig. 7. Schematic model of ASK1-mediated glial interaction during neuroinflammation. (*Left*) ASK1 signaling in microglia plays a pathogenic role in the early stage of EAE: ASK1 signaling in microglia polarizes microglia toward a proinflammatory state (red arrow). Proinflammatory microglia induce proinflammatory astrocytes (red arrow), produce CCL2 (blue arrow), and recruit macrophages into the CNS (orange arrow). ASK1 signaling in macrophages promotes macrophages to be in a proinflammatory state. ASK1-mediated activation of these glial cells causes severe inflammation. (*Right*) ASK1 signaling in astrocytes plays a pathogenic role in the later stage of EAE: ASK1 signaling in astrocytes promotes secretion of cytokines and chemokines to induce proinflammatory microglia and recruit macrophages into the CNS. Proinflammatory microglia induce proinflammatory astrocytes; and therefore we propose a glial interaction cycle, in which astrocytes and microglia activate each other in an ASK1-dependent manner. ASK1-mediated activation of these glial cells causes sustained inflammation.

successful in future and it will help to confirm the role of ASK in macrophages using macrophage-specific CKO mice. Furthermore, we could not distinguish which populations of macrophages were affected by ASK1 deletion. Future studies include use of multiplex in situ hybridization approaches or related approaches to localize and reveal changes in specific populations and spatial information to elucidate the role of ASK1 in more detail.

Microglia–astrocyte interactions play critical roles in CNS inflammation (42). A newly identified subtype of A1 reactive astrocytes can be induced by proinflammatory microglia, and such glial interactions may subsequently affect oligodendrocyte differentiation and survival (17, 43, 44). In our study, we showed that the number of A1 astrocytes in ASK1^{CX3CR1} KO EAE mice was reduced compared with the number observed in WT EAE mice. In addition, our in vitro study demonstrated that the number of A1 astrocytes decreased when astrocytes were stimulated with MCM from ASK1 KO microglia compared with those stimulated with MCM from WT microglia (Fig. 4*B*). Meanwhile, ASK1 deficiency in astrocytes had no effects on the induction of the A1 phenotype (*SI Appendix*, Fig. S13). These data suggest that the induction of A1 astrocytes during EAE is mediated at least partly via ASK1 signaling in microglia. Recent study demonstrated that chronically activated microglia suppress the differentiation of oligodendrocyte progenitor cells and axon myelination (45), thus suggesting a new glial relationship among microglia, astrocytes, and oligodendrocytes in MS/EAE. Further

in vivo validation and functional studies are needed to confirm the proposed mechanism.

During neuroinflammation, astrocyte-derived cytokines/chemokines play important roles in the recruitment of immune cells into the CNS, the induction of inflammatory responses, and later-stage disease mechanisms such as chronic demyelination and axonal loss (46–48). We demonstrated that ASK1 signaling in astrocytes drives proinflammatory gene expression, some of which is involved in the recruitment or activation of microglia/macrophages, but only in the later stage of EAE. In particular, we found that astrocytic CCL2 expression, which is up-regulated via ASK1 signaling (21), is significantly increased in the later stage of EAE, but this increase was almost completely abolished in the absence of ASK1 (Fig. 6). These findings clearly suggest an important pathogenic role of ASK1-mediated regulation of CCL2 expression in the later stage of EAE, although follow-up studies, such as CCL2 deletion in astrocytes in the later stage of EAE using the *CCL2:hGFAP-CreERT2* mouse strain, may be helpful to confirm this conclusion. Recent advances in genomic tools facilitated progress in understanding the roles of astrocytes in MS pathogenesis (49). Transcriptome analysis revealed a few key genes that are expressed in astrocytes and associated with proinflammatory astroglial activation in EAE. For example, glycolipid lactosylceramide (LacCer), a member of the glycosphingolipid family and synthesized by β-1,4-galactosyltransferase 6 (B4GALT6) in astrocytes, was up-regulated particularly at the later stage of

Guo et al.
ASK1 signaling regulates phase-specific glial interactions during neuroinflammation

PNAS | 9 of 12
https://doi.org/10.1073/pnas.2103812119

EAE and promoted neurodegeneration (14). A recent study into heterogeneity of astrocytes in EAE and MS by single-cell RNA sequencing revealed the importance of environmental factors that activate astrocytes (16, 47, 50) The fact that ASK1 deficiency in astrocytes reduced the severity of EAE only in the later stage of the disease suggests that there was a change in environment at the lesion site from early to later stage that affected ASK1 signaling. Our future studies include identification of the factors responsible for this change, which could contribute to further understanding of mechanisms involved in acute and chronic inflammation. It is important to note that although the *GFAP-Cre* mouse strain used in the present study has been frequently used for astrocyte-specific inactivation of genes of interest, there is some degree of leakiness in other cell types such as neurons (51). Using inducible *Cre* driver transgenic mouse lines such as *hGFAP-CreERT2* showing high astrocyte-specific *Cre* expression would further validate our findings (52, 53).

ASK1 has been implicated in various human diseases, including Alzheimer's disease and diabetes; thus inhibition of ASK1 has been an attractive strategy for these disorders. Recently, selonsertib, an ASK1 inhibitor, went through clinical trials for the treatment of nonalcoholic steatohepatitis (NASH). Disappointingly, trials failed to reach the primary efficacy endpoint (54, 55); however, it is possible that selonsertib may be a suitable candidate for drug repositioning and may show efficacy in treatment of various other disease conditions.

In summary, our results demonstrate that ASK1 signaling regulates glial cell interactions and drives CNS inflammation, suggesting that ASK1 may be a good therapeutic target for neurodegenerative diseases, including MS. Further studies of ASK1 signaling that disrupt glial cell homeostasis may provide detailed understanding of the cell-type–specific changes within the pathological environment during neuroinflammation.

Materials and Methods

Animals. Mice homozygous for the ASK1 floxed allele (ASK1$^{flox/flox}$) on a C57BL/6J background were generated as previously described (22). *Lck-Cre*[+] (56), *Cd11c-Cre*[+] (57), *LysM-Cre*[+] (58), *GFAP-Cre*[+] (59), and *CX3CR1*^{CreER} mice (25) were used to create conditional ASK1 KO mice. Female C57BL/6J, conventional, and conditional ASK1 KO mice were maintained at the animal facilities of the Tokyo Metropolitan Institute of Medical Science and were 6 to 8 wk of age at the time of immunization. RiboTag mice (37) and tdTomato mice (60) were purchased from The Jackson Laboratory. The animals were treated in accordance with the Tokyo Metropolitan Institute of Medical Science Guidelines for the Care and Use of Animals. All animal experiments were approved by the Institutional Animal Care and Use Committee of the Tokyo Metropolitan Institute of Medical Science (18041).

EAE Induction and Clinical Scoring. EAE was induced in mice with MOG$_{35-55}$ peptide (MEVGWRSPFSRVVHLYRNGK) as previously reported (61). Briefly, mice were subcutaneously injected with 100 μg of MOG$_{35-55}$ mixed with 500 μg of heat-killed *Mycobacterium tuberculosis* H37RA (Difco) emulsified in complete Freund's adjuvant. Each mouse also received intraperitoneal injections of 400 ng pertussis toxin (Seikagaku) immediately and 48 h after the immunization. Clinical signs were scored daily as follows: 0, no clinical signs; 1, loss of tail tonicity; 2, flaccid tail; 3, impairment of righting reflex; 4, partial hind limb paralysis; 5, complete hind limb paralysis; 6, partial body paralysis; 7, partial forelimb paralysis; 8, complete forelimb paralysis or moribund; and 9, death.

Histopathology and Quantification. Mice were anesthetized by an intraperitoneal injection of sodium pentobarbital, perfused transcardially with saline followed by 4% paraformaldehyde in 0.1 M phosphate buffer containing 0.5% picric acid. Optic nerves and lumbar spinal cords were removed, postfixed, and processed as previously reported (21, 62). Briefly, optic nerves were embedded in paraffin wax, cut into 7-μm-thick sections, and stained with LFB followed by H&E staining. Spinal cords were embedded in paraffin wax or optimal cutting temperature (OCT) compound (Tissue-Tek), and sections (10 μm) were cut coronally and collected on MAS-coated slides (Matsunami) that are silane-coated slides with improved hydrophilicity and adhesion. For pathological study, sections were stained with LFB followed by H&E. Immunohistochemistry

was performed using the following primary antibodies: mouse anti-CCL2 (1:500; MABN712, Merck Millipore), mouse anti-iNOS (1:100; 610328, BD Biosciences), rat anti-CD86 (1:200; 550542, BD Biosciences), rabbit anti-IL1β (1:100; bs-0812R, Bioss), rabbit anti-TNFα (1:100; bs-2081R, Bioss), goat anti-GFAP (1:200; sc-6170, Santa Cruz), rabbit anti-GFAP (1:200; 12389s, Cell Signaling), goat anti-iba1 (1:400; ab5076, Abcam), rabbit anti-TMEM119 (1:500; ab209064, Abcam), rabbit anti-C3d (1:200; A0063, DAKO), rabbit anti-ASK1 (1:1,000; ab45178, Abcam), rabbit anti-pASK1 (1:200; bs-3031R, Bioss), mouse anti–p-p38 (1:500; 612280, BD Biosciences), goat anti-CD31 (1:100; AF3628, R&D Systems), mouse anti-fibronectin (1:200; F7387, Merck Millipore), rabbit anti-NeuN (1:200; 24307s, Cell Signaling Technology), and rat anti-CD3 (1:200; MCA500GT, Bio-Rad). Stained sections were examined using a microscope (BX51; Olympus) equipped with Plan Fluor objectives (Olympus) connected to a DP70 camera (Olympus) or Keyence BZ-X800. Images were processed and viewed using DP manager (v2.2.1.195; Olympus) software or BZ-H3A application software (Keyence). For quantification, the intensities of the whole area (ventral funiculus [VF], lateral funiculus [LF], and dorsal funiculus [DF] of the white matter or gray matter) were measured using NIH ImageJ software 1.43u (available at https://rsb.info.nih.gov/ij/index.html), or immunopositive cells in the whole area as above were counted in three sections per mouse. The number of mice examined is shown in each figure legend.

Electron Microscopy. Electron microscopy was performed on mouse optic nerve sections. EAE mice at d30 were transcardially perfused with a 0.9% NaCl solution followed by 2% paraformaldehyde and 2.5% glutaraldehyde in 0.1 M phosphate buffer (pH 7.4). Optic nerves were harvested and stored in the same fixative solution at 4 °C. The following day, after being rinsed several times in 0.1 M cacodylate buffer (CB) with 4.5% sucrose to remove excess aldehyde, the samples were postfixed in 2% osmium tetroxide in 0.1 M CB for 2 h at 4 °C with constant agitation, dehydrated by serial dilutions of ethanol followed by propylene oxide, and then infiltrated with and embedded in epoxy resin (EPON 812, TAAB Laboratory and Microscopy). All samples were oriented for cross-section analysis. Semithin sections (1 μm thick) were stained with toluidine blue before collection for electron microscopy analysis. Ultrathin sections (70 nm thick) with silver and/or gray interference color were cut and placed in formvar-coated one-slot grids. The grids were stained with uranyl acetate and lead citrate and used for ultrastructural evaluation. All images were collected using a transmission electron microscope (JEM-1400, JEOL).

Microarray Analysis. Total RNA extracted from the spinal cords was purified using a RNeasy Lipid Tissue Kit (Qiagen). The quality of RNA was assessed with a 2100 Bioanalyzer (Agilent Technologies). Cy3-labeled cRNA was prepared using a Low Input Quick Amp Labeling Kit according to the manufacturer's protocol (Agilent Technologies). Samples were hybridized to the Mouse Gene Expression v2 Microarray (G4846A; Agilent Technologies), washed, and then scanned using a SureScan Microarray Scanner (Agilent Technologies). The microarray images were analyzed with Feature Extraction software (Agilent Technologies). Data from each microarray analysis were normalized by global normalization. These procedures were performed in the microarray facility in the Tokyo Metropolitan Institute of Medical Science.

RNA Immunoprecipitation. Immunoprecipitation using mouse monoclonal anti-HA antibody (1:50; clone 16B12, BioLegend) were performed as previously reported with minor modification (37).

qPCR. qPCR was performed using the MyiQ real-time PCR system (Bio-Rad) with Thunderbird SYBR qPCR Mix (Toyobo) as previously reported. The primer sets used are listed in *SI Appendix*, Table 1. Gene expression levels were normalized to GAPDH.

SCH Preparation. Lumbar spinal cords (L1–L3) of WT EAE mice on d17 and d30 were isolated, placed into sterile dishes, and rinsed with ice-cold phosphate buffered saline (PBS). Spinal cords were homogenized in serum-free Dulbecco's Modified Eagle Medium (DMEM) (1 mL) on ice, centrifuged at 12,000 rpm for 15 min at 4 °C, and the supernatants were obtained as SCHs. SCHs were then quantified by Bradford MX (25 μg/mL to 2,000 μg/mL; 10 μL sample/ bovine serum albumin (BSA) in 600 μL), and the concentrations were adjusted to 200 μg/mL. SCHs were aliquoted and stored at −30 °C until use.

Primary Cell Cultures. Primary astrocyte and microglia cultures were prepared as previously reported (21, 63). Briefly, the cells were isolated from cerebral cortices of 1- to 3-d-old WT or ASK1 KO mice and seeded on a 75-cm^2 tissue culture flask. Complete confluence was reached in 7 to 10 d. Flasks were then shaken for 1 h (150 rpm at 37 °C) in a temperature-controlled shaker to loosen microglia and oligodendrocytes from the more adherent astrocytes. These less adherent cells were plated for 2 h and then lightly shaken to remove

oligodendrocytes from the more adherent microglia. The microglia were used for M1/M2 polarization experiments, immunoblot analysis, or for preparation of MCM. After shaking to remove microglia and oligodendrocytes, astrocytes were recovered by trypsinization, seeded in 96-well plates (5×10^4 cells/well), and cultured for 2 d. WT or ASK1 KO astrocytes were treated with MCM prepared from WT or ASK1 KO microglia to investigate the effects of ASK1 deficiency on the inducing of a A1 astrocyte.

To generate BMDMs, the bone marrow cells from femurs and tibias of WT or ASK1 KO mice were harvested and cultured in RPMI supplemented with 10 ng/mL macrophage colony-stimulating factor (M-CSF). The culture medium was replaced every 2 d. On day 7 in culture, the cells were harvested and used for M1/M2 polarization experiments. SuperPrep Cell Lysis and RT Kit for qPCR (Toyobo) were used for the preparation of cDNA.

MCM Preparation. Primary microglia cultures derived from WT or ASK1 KO mice were seeded in 3.5-cm dishes (1×10^6 cells/dish) and incubated 24 h followed by stimulation with LPS (100 ng/mL) for 3 h. Cells were washed three times with serum-free media and cultured in 1 mL of medium containing 1% fetal bovine serum for 24 h. The culture medium was collected and centrifuged. The supernatants were then used as conditioned medium, aliquoted, and stocked at $-80\,°C$ until use.

Statistical Analysis. Statistics were performed using JMP 13 software (SAS Institute). Data are represented as mean $\pm$ SEM. Data significance was determined using two-tailed Student's *t* tests, or one-way ANOVA with Tukey–Kramer post hoc test. Statistical significance is reported as significant at $P < 0.05$.

Data Availability. All study data are included in the article and/or supporting information.

1. Y. Kawarazaki, H. Ichijo, I. Naguro, Apoptosis signal-regulating kinase 1 as a therapeutic target. *Expert Opin. Ther. Targets* **18**, 651–664 (2014).
2. C. Sakauchi, H. Wakatsuki, H. Ichijo, K. Hattori, Pleiotropic properties of ASK1. *Biochim. Biophys. Acta, Gen. Subj.* **1861** (1 Pt A), 3030–3038 (2017).
3. C. Harada et al., Role of apoptosis signal-regulating kinase 1 in stress-induced neural cell apoptosis in vivo. *Am. J. Pathol.* **168**, 261–269 (2006).
4. T. Katome et al., Inhibition of ASK1-p38 pathway prevents neural cell death following optic nerve injury. *Cell Death Differ.* **20**, 270–280 (2013).
5. T. Fujisawa et al., The ASK1-specific inhibitors K811 and K812 prolong survival in a mouse model of amyotrophic lateral sclerosis. *Hum. Mol. Genet.* **25**, 245–253 (2016).
6. Y. Hasegawa, K. Toyama, K. Uekawa, H. Ichijo, S. Kim-Mitsuyama, Role of ASK1/p38 cascade in a mouse model of Alzheimer's disease and brain aging. *J. Alzheimers Dis.* **61**, 259–263 (2018).
7. A. Ray, N. Sehgal, S. Karunakaran, G. Rangarajan, V. Ravindranath, MPTP activates ASK1-p38 MAPK signaling pathway through TNF-dependent Trx1 oxidation in parkinsonism mouse model. *Free Radic. Biol. Med.* **87**, 312–325 (2015).
8. X. Guo, K. Namekata, A. Kimura, C. Harada, T. Harada, ASK1 in neurodegeneration. *Adv. Biol. Regul.* **66**, 63–71 (2017).
9. C. S. Constantinescu, N. Farooqi, K. O'Brien, B. Gran, Experimental autoimmune encephalomyelitis (EAE) as a model for multiple sclerosis (MS). *Br. J. Pharmacol.* **164**, 1079–1106 (2011).
10. V. E. Miron et al., M2 microglia and macrophages drive oligodendrocyte differentiation during CNS remyelination. *Nat. Neurosci.* **16**, 1211–1218 (2013).
11. C. Liu et al., Targeting the shift from M1 to M2 macrophages in experimental autoimmune encephalomyelitis mice treated with fasudil. *PLoS One* **8**, e54841 (2013).
12. F. Chu et al., The roles of macrophages and microglia in multiple sclerosis and experimental autoimmune encephalomyelitis. *J. Neuroimmunol.* **318**, 1–7 (2018).
13. H. Lassmann, Mechanisms of white matter damage in multiple sclerosis. *Glia* **62**, 1816–1830 (2014).
14. L. Mayo et al., Regulation of astrocyte activation by glycolipids drives chronic CNS inflammation. *Nat. Med.* **20**, 1147–1156 (2014).
15. R. Y. Kim et al., Astrocyte CCL2 sustains immune cell infiltration in chronic experimental autoimmune encephalomyelitis. *J. Neuroimmunol.* **274**, 53–61 (2014).
16. M. A. Wheeler et al., Environmental control of astrocyte pathogenic activities in CNS inflammation. *Cell* **176**, 581–596.e18 (2019).
17. S. A. Liddelow et al., Neurotoxic reactive astrocytes are induced by activated microglia. *Nature* **541**, 481–487 (2017).
18. S. P. Yun et al., Block of A1 astrocyte conversion by microglia is neuroprotective in models of Parkinson's disease. *Nat. Med.* **24**, 931–938 (2018).
19. C. Escartin et al., Reactive astrocyte nomenclature, definitions, and future directions. *Nat. Neurosci.* **24**, 312–325 (2021).
20. P. Hasel, I. V. L. Rose, J. S. Sadick, R. D. Kim, S. A. Liddelow, Neuroinflammatory astrocyte subtypes in the mouse brain. *Nat. Neurosci.* **24**, 1475–1487 (2021).
21. X. Guo et al., Regulation of the severity of neuroinflammation and demyelination by TLR-ASK1-p38 pathway. *EMBO Mol. Med.* **2**, 504–515 (2010).
22. K. Hattori et al., ASK1 signalling regulates brown and beige adipocyte function. *Nat. Commun.* **7**, 11158 (2016).
23. A. Boroujerdi, J. V. Welser-Alves, R. Milner, Extensive vascular remodeling in the spinal cord of pre-symptomatic experimental autoimmune encephalomyelitis mice; increased vessel expression of fibronectin and the $\alpha 5\beta 1$ integrin. *Exp. Neurol.* **250**, 43–51 (2013).
24. D. Davalos et al., Fibrinogen-induced perivascular microglial clustering is required for the development of axonal damage in neuroinflammation. *Nat. Commun.* **3**, 1227 (2012).
25. T. Goldmann et al., A new type of microglia gene targeting shows TAK1 to be pivotal in CNS autoimmune inflammation. *Nat. Neurosci.* **16**, 1618–1626 (2013).
26. R. Fekete et al., Microglia control the spread of neurotropic virus infection via P2Y12 signalling and recruit monocytes through P2Y12-independent mechanisms. *Acta Neuropathol.* **136**, 461–482 (2018).
27. R. N. Dogan, A. Elhofy, W. J. Karpus, Production of CCL2 by central nervous system cells regulates development of murine experimental autoimmune encephalomyelitis through the recruitment of TNF- and iNOS-expressing macrophages and myeloid dendritic cells. *J. Immunol.* **180**, 7376–7384 (2008).
28. M. Jin, E. Jang, K. Suk, Lipocalin-2 acts as a neuroinflammatogen in lipopolysaccharide-injected mice. *Exp. Neurobiol.* **23**, 155–162 (2014).
29. M. R. Elmore et al., Colony-stimulating factor 1 receptor signaling is necessary for microglia viability, unmasking a microglia progenitor cell in the adult brain. *Neuron* **82**, 380–397 (2014).
30. J. C. Nissen, K. K. Thompson, B. L. West, S. E. Tsirka, Csf1R inhibition attenuates experimental autoimmune encephalomyelitis and promotes recovery. *Exp. Neurol.* **307**, 24–36 (2018).
31. Y. Okamura et al., The extra domain A of fibronectin activates Toll-like receptor 4. *J. Biol. Chem.* **276**, 10229–10233 (2001).
32. R. Milner et al., Fibronectin- and vitronectin-induced microglial activation and matrix metalloproteinase-9 expression is mediated by integrins alpha5beta1 and alphavbeta5. *J. Immunol.* **178**, 8158–8167 (2007).
33. S. Bussini et al., Heparan sulfate proteoglycan induces the production of NO and TNF-alpha by murine microglia. *Immun. Ageing* **2**, 11 (2005).
34. M. Moreno et al., Conditional ablation of astroglial CCL2 suppresses CNS accumulation of M1 macrophages and preserves axons in mice with MOG peptide EAE. *J. Neurosci.* **34**, 8175–8185 (2014).
35. L. Izikson, R. S. Klein, I. F. Charo, H. L. Weiner, A. D. Luster, Resistance to experimental autoimmune encephalomyelitis in mice lacking the CC chemokine receptor (CCR)2. *J. Exp. Med.* **192**, 1075–1080 (2000).
36. D. R. Huang, J. Wang, P. Kivisakk, B. J. Rollins, R. M. Ransohoff, Absence of monocyte chemoattractant protein 1 in mice leads to decreased local macrophage recruitment and antigen-specific T helper cell type 1 immune response in experimental autoimmune encephalomyelitis. *J. Exp. Med.* **193**, 713–726 (2001).
37. E. Sanz et al., Cell-type-specific isolation of ribosome-associated mRNA from complex tissues. *Proc. Natl. Acad. Sci. U.S.A.* **106**, 13939–13944 (2009).
38. S. David, A. Kroner, Repertoire of microglial and macrophage responses after spinal cord injury. *Nat. Rev. Neurosci.* **12**, 388–399 (2011).
39. M. W. Salter, B. Stevens, Microglia emerge as central players in brain disease. *Nat. Med.* **23**, 1018–1027 (2017).
40. A. I. Ramirez et al., The role of microglia in retinal neurodegeneration: Alzheimer's disease, Parkinson, and glaucoma. *Front. Aging Neurosci.* **9**, 214 (2017).
41. S. G. Utz et al., Early fate defines microglia and non-parenchymal brain macrophage development. *Cell* **181**, 557–573.e18 (2020).
42. R. M. Ransohoff, M. A. Brown, Innate immunity in the central nervous system. *J. Clin. Invest.* **122**, 1164–1171 (2012).
43. E. M. Gibson et al., Methotrexate chemotherapy induces persistent tri-glial dysregulation that underlies chemotherapy-related cognitive impairment. *Cell* **176**, 43–55.e13 (2019).
44. E. Traiffort, A. Kassoussi, A. Zahaf, Y. Laouarem, Astrocytes and microglia as major players of myelin production in normal and pathological conditions. *Front. Cell. Neurosci.* **14**, 79 (2020).
45. J. Wang et al., Robust myelination of regenerated axons induced by combined manipulations of GPR17 and microglia. *Neuron* **108**, 876–886.e4 (2020).
46. R. R. Voskuhl et al., Reactive astrocytes form scar-like perivascular barriers to leukocytes during adaptive immune inflammation of the CNS. *J. Neurosci.* **29**, 11511–11522 (2009).
47. V. Rothhammer et al., Microglial control of astrocytes in response to microbial metabolites. *Nature* **557**, 724–728 (2018).

Guo et al.
ASK1 signaling regulates phase-specific glial interactions during neuroinflammation

PNAS | 11 of 12
https://doi.org/10.1073/pnas.2103812119

48. R. Brambilla, The contribution of astrocytes to the neuroinflammatory response in multiple sclerosis and experimental autoimmune encephalomyelitis. *Acta Neuropathol.* **137**, 757–783 (2019).

49. M. A. Wheeler, F. J. Quintana, Regulation of astrocyte functions in multiple sclerosis. *Cold Spring Harb. Perspect. Med.* **9**, a029009 (2019).

50. M. A. Wheeler *et al.*, MAFG-driven astrocytes promote CNS inflammation. *Nature* **578**, 593–599 (2020).

51. Y. M. Park, H. Chun, J. I. Shin, C. J. Lee, Astrocyte specificity and coverage of hGFAP-CreERT2 [Tg(GFAP-Cre/ERT2)13Kdmc] mouse line in various brain regions. *Exp. Neurobiol.* **27**, 508–525 (2018).

52. Y. M. Ganat *et al.*, Early postnatal astroglial cells produce multilineage precursors and neural stem cells in vivo. *J. Neurosci.* **26**, 8609–8621 (2006).

53. P. G. Hirrlinger, A. Scheller, C. Braun, J. Hirrlinger, F. Kirchhoff, Temporal control of gene recombination in astrocytes by transgenic expression of the tamoxifen-inducible DNA recombinase variant CreERT2. *Glia* **54**, 11–20 (2006).

54. R. Loomba *et al.*, GS-US-384-1497 Investigators, The ASK1 inhibitor selonsertib in patients with nonalcoholic steatohepatitis: A randomized, phase 2 trial. *Hepatology* **67**, 549–559 (2018).

55. S. A. Harrison *et al.*, STELLAR-3 and STELLAR-4 Investigators, Selonsertib for patients with bridging fibrosis or compensated cirrhosis due to NASH: Results from randomized phase III STELLAR trials. *J. Hepatol.* **73**, 26–39 (2020).

56. Y. Takahama *et al.*, Functional competence of T cells in the absence of glycosylphosphatidylinositol-anchored proteins caused by T cell-specific disruption of the Pig-a gene. *Eur. J. Immunol.* **28**, 2159–2166 (1998).

57. M. L. Caton, M. R. Smith-Raska, B. Reizis, Notch-RBP-J signaling controls the homeostasis of CD8- dendritic cells in the spleen. *J. Exp. Med.* **204**, 1653–1664 (2007).

58. D. R. Herbert *et al.*, Alternative macrophage activation is essential for survival during schistosomiasis and downmodulates T helper 1 responses and immunopathology. *Immunity* **20**, 623–635 (2004).

59. C. Harada *et al.*, Glia- and neuron-specific functions of TrkB signalling during retinal degeneration and regeneration. *Nat. Commun.* **2**, 189 (2011).

60. L. Madisen *et al.*, A robust and high-throughput Cre reporting and characterization system for the whole mouse brain. *Nat. Neurosci.* **13**, 133–140 (2010).

61. I. Mendel, N. Kerlero de Rosbo, A. Ben-Nun, A myelin oligodendrocyte glycoprotein peptide induces typical chronic experimental autoimmune encephalomyelitis in H-2b mice: Fine specificity and T cell receptor V beta expression of encephalitogenic T cells. *Eur. J. Immunol.* **25**, 1951–1959 (1995).

62. X. Guo *et al.*, Spermidine alleviates severity of murine experimental autoimmune encephalomyelitis. *Invest. Ophthalmol. Vis. Sci.* **52**, 2696–2703 (2011).

63. X. Guo *et al.*, Inhibition of glial cell activation ameliorates the severity of experimental autoimmune encephalomyelitis. *Neurosci. Res.* **59**, 457–466 (2007).